analytical chemistry

Article

Cite This: *Anal. Chem.* 2019, 91, 2216–2223

pubs.acs.org/ac

Malaria Detection by Third-Harmonic Generation Image Scanning Cytometry

Alexei Kazarine,[†] Fadi Baakdah,[‡] Angelica A. Gopal,[†] Wellington Oyibo,[§] Elias Georges,[‡] and Paul W. Wiseman*[,†,∥]

[†]Department of Chemistry, McGill University, 801 Sherbrooke Street West, Montreal, Quebec H3A 0B8, Canada

[‡]Institute of Parasitology, McGill University, Sainte Anne de Bellevue, Quebec H9X 3 V9, Canada

[§]ANDI Centre of Excellence for Malaria Diagnosis, College of Medicine, University of Lagos, Idi-Araba, Lagos 100254, Nigeria

[∥]Department of Physics, McGill University, 3600 University Street, Montreal, Quebec H3A 2T8, Canada

Supporting Information

ABSTRACT: Despite global efforts aimed at its elimination, malaria is still a significant health concern in many countries across the world. The disease is caused by blood-borne parasites, *Plasmodium* species, and is transmitted by female *Anopheles* mosquitoes and presents with generic febrile symptoms that are challenging to diagnose clinically. To adequately tackle this issue, an effective detection method is required for screening potential malaria patients for infection. To this day, the gold standard for malaria detection remains basic light microscopy of Giemsa-stained patient blood smears to first enable detection and manual counting to determine the parasite density by a microscopist. While effective at detecting parasites, this method requires both significant time and skilled personnel. As an alternate approach, we propose a new malaria detection method that we call third-harmonic generation image scanning cytometry (THGISC) based on the combination of third-harmonic generation imaging, high-speed motorized scanning, and automated software processing. Third-harmonic generation (THG) is a nonlinear optical process in which the frequency of incident photons is tripled within the sample material. We have previously demonstrated that hemozoin, a metabolic byproduct of the malaria parasite, presents a significant THG signal. We now present a practical approach that uses the selectivity of this contrast mechanism to perform label-free image scanning cytometry of patient blood smears for automated malaria detection. In this work, we applied this technique to lab-cultured parasites and parasites in whole blood obtained from malaria patients. We also compared its effectiveness to parasite counts obtained by classical methods. The ability to easily and rapidly determine parasitemia by THG offers potential not only for the easy confirmation of malaria diagnoses following symptoms, but also the tracking of treatment progress in existing patients, potentially allowing physicians to adjust medication and dosage for each individual.

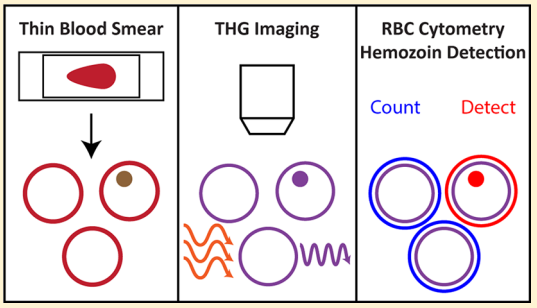

To this day, malaria remains a significant global public health issue. This infectious disease is caused by *Plasmodium* species, blood-borne apicomplexan parasites transmitted by mosquitoes, with most cases and deaths caused by *Plasmodium falciparum*.[1] In 2017, the World Health Organization (WHO) reported over 216 million cases of infection, with over 90% occurring in Africa.[2] It is estimated that malaria causes over a hundred thousand deaths each year. The infection begins from sporozoites injected into the bloodstream during the mosquito's blood meal.[3] This infective motile stage of the parasite travels to the liver where it begins reproducing asexually, releasing merozoites into the bloodstream. These merozoites proceed to infect erythrocytes to replicate, consuming the hemoglobin contained within, and enter the ring stage. The rings then mature to become trophozoites. After rapid growth within the red blood cell (RBC), they undergo multiple asexual fission (schizogony) developing into a schizont that eventually results in hemolysis and release of merozoites to continue the parasitic lifecycle. During hemolysis, the patient presents with general febrile symptoms, making clinical diagnosis difficult.[4,5] While the disease is curable, early and accurate confirmation of malaria parasites in suspected patients is critical for effective case management of malaria to prevent the onset of severe malaria that may be fatal.

The current gold standard for malaria detection is light microscopy[6] that requires the preparation of Giemsa-stained blood smears that are then examined by a trained technician who would have to skillfully view the fields of the smear to detect or negate the presence of the parasite. Thick blood smears allow for more sensitive parasite detection, while thin blood smears permit more precise determination of the

Received: October 18, 2018
Accepted: January 2, 2019
Published: January 2, 2019

DOI: 10.1021/acs.analchem.8b04791
Anal. Chem. 2019, 91, 2216–2223

Plasmodium species. However, this method presents several drawbacks, including the need for trained and experienced personnel, low detection sensitivity for cases of low parasitemia, and the subjective nature of manual observation. A variety of alternative malaria diagnostic techniques have now been developed including fluorescence microscopy,[7] point-of-care rapid diagnostic tests[8] (RDT) based on antigen detection, nucleic acid based analyses,[9] microfluidic devices,[10] and other sensors.[11] While these methods show significant promise, the WHO still recommends the use of light microscopy as the diagnostic tool for potential malaria cases[2] in addition to malaria RDTs.

Other detection methods have been elaborated based on the detection of hemozoin,[12] a biocrystalline byproduct of the *Plasmodium* parasite's digestion of hemoglobin, instead of direct parasite detection. This metabolic byproduct is characteristic of malaria infection and is presently being researched as a biomarker for malaria detection[13] as well as a potential target for antimalarial drugs. Hemozoin's nature as a biological crystal endows it interesting optical properties that can be exploited for its detection. Several potential malaria diagnostic methods have now been demonstrated, including the use of cell-phone-based polarized light microscopy to exploit its birefringence[14] and an acoustic method based on the production of nanobubbles generated by its interaction with ultrafast laser pulses.[15,16] Another technique based on simple in vivo UV−vis absorption spectroscopy of hemozoin has also been reported.[17]

Another remarkable optical property of hemozoin is its significant third-order nonlinear optical susceptibility resulting in efficient third-harmonic generation (THG). THG is a nonlinear coherent optical process in which three photons of incident light combine to form one photon at one-third of the excitation wavelength. This process mainly occurs at interfaces between materials presenting different refractive indexes or third-order nonlinear susceptibilities.[18] THG imaging provides a simple yet powerful contrast method that does not require any form of external labeling. We have previously demonstrated that hemozoin presents a highly specific THG signal when illuminated with near-infrared ultrafast pulses.[19] The method was demonstrated on both cultured *Plasmodium* parasites and synthetic hematin anhydride crystals, but its practical effectiveness has not yet been established.[20]

In the development of an effective and practical implementation of THG-based malaria detection, a high-throughput approach is desired to maximize detection chances and minimize time-to-answer. One such approach could be its implementation into flow cytometry. However, as THG is an interface effect that requires scanning with a diffraction-limited laser beam, it is not directly compatible with flow cytometry instrumentation which typically utilizes a widefield configuration. A more practical approach to THG-based malaria detection is its implementation in the form of image scanning cytometry. Unlike flow cytometry, image scanning cytometry relies on automated rapid scanning of microscopy slide areas to perform single-cell optical measurements on a high-throughput level.[21,22] One additional advantage of imaged-based cytometry over standard flow cytometry is the ability to obtain detailed data for each imaged cell, including morphological data such as cell size.[23] Overall, while image scanning cytometry does present a lower throughput than flow cytometry, it is presently the favored option when it comes to THG cytometry due to the unique interface-based nature of this contrast mechanism.

In this work, we combined THG imaging with motorized scanning and easy-to-use processing software to establish a new method for malaria detection that we call third-harmonic generation image scanning cytometry (THGISC) (Figure 1).

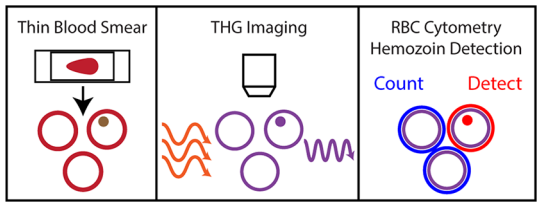

Figure 1. Methodology schematic of malaria detection by THG image scanning cytometry.

Using a single detection channel, we can locate both red blood cells and *Plasmodium* parasites via their hemoglobin and hemozoin crystals, respectively. This method enables screening at the single red blood cell level to rapidly and effectively determine parasitemia in whole patient blood, label-free. Thanks to the specificity of the THG signal and the use of automated image analysis, malaria detection using THGISC does not require prior user experience or skill. We have tested the method on both cultured *P. falciparum* parasites at several erythrocytic lifecycle stages and whole-blood samples obtained from confirmed malaria patients. Method performance was compared using two-photon fluorescence (TPF) microscopy of fluorescent nuclear stains using the same imaging system for the cultured parasites. Classical light microscopy was used to independently verify parasitemia for the patient study.

METHODS

***P. falciparum* Asexual Blood Stages Cultivation.** *P. falciparum* 3D7-H strain was maintained in a continuous synchronous culture as described previously by Trager and Jensen[24] with a few modifications. Culture reagents were obtained from ThermoFisher Scientific, Massachusetts, unless stated otherwise. Briefly, parasites were cultivated in RPMI 1640 media supplemented with L-glutamine and HEPES in 10% human plasma and A+ human erythrocytes (The Interstate Blood Bank Inc., Tennessee) in a maintained packed cell volume of 2%. They were synchronized with 5% sorbitol (MilliporeSigma, Ontario, Canada), and each stage was collected at 8% from rings, trophozoites, and schizonts. Once the parasites reached 8% they were washed with PBS and fixed in 4% paraformaldehyde (electron microscopy grade, Electron Microscopy Sciences, Pennsylvania) in PBS.

Patient Blood Collection from Clinical Cases and Parasitemia Determination. Blood samples were collected from patients that presented with malaria-related symptoms who consented to participating in an ongoing malaria research in Ikorodu, Lagos, Nigeria. The study protocol was approved by the Ethics Committee of the College of Medicine, University of Lagos, Lagos, Nigeria. In summary, 3 mL of venous blood was collected from patients and stored in a 5 mL EDTA blood bottle that was gently rotated to ensure the collected blood mixed with the anticoagulant. Two thin and thick malaria blood films (MBFs) were prepared on the same slide and stained with Giemsa using standard protocol.

The stained MBFs were read independently by two WHO grade I certified microscopists who confirmed the presence or absence of *Plasmodium* species (detection), speciated into

DOI: 10.1021/acs.analchem.8b04791
Anal. Chem. 2019, 91, 2216−2223

different species of *Plasmodium* species, reported the stage of the parasites, and enumerated the parasites in thick film using standard procedures. Where there was discordance in parasite detection and counts, a third microscopist that served as an arbiter reread the MBF to resolve the discordant result. The *Plasmodium* parasites seen were counted against a minimum of 500 leucocytes, while 200 oil immersion fields were scanned to declare an MBF negative. Parasite density was computed using an estimated 8000 white blood cells and reported as parasites per microliter of blood from parasites in thick film preparation.

Sample Preparation from Cultured *Plasmodium* Parasites. Thin blood smears were prepared from parasites cultured and synchronized at three different lifecycle stages: ring, trophozoite, and schizont. Samples were separately stained with two fluorescent nuclear stains: acridine orange (MilliporeSigma, Ontario, Canada) or DAPI (4′,6-diamidino-2-phenylindole, ThermoFisher Scientific, Massachusetts, U.S.A.) for verification. Blood smears were also prepared from whole-blood samples obtained from malaria patients after dilution in phosphate-buffered saline (DPBS, ThermoFisher Scientific, Massachusetts, U.S.A.) by 50% to ensure thin films. Samples were rehydrated and mounted on coverslips immediately prior to imaging.

Experimental Setup. THGISC was conducted using a customized multiphoton imaging system (Figure 2). The

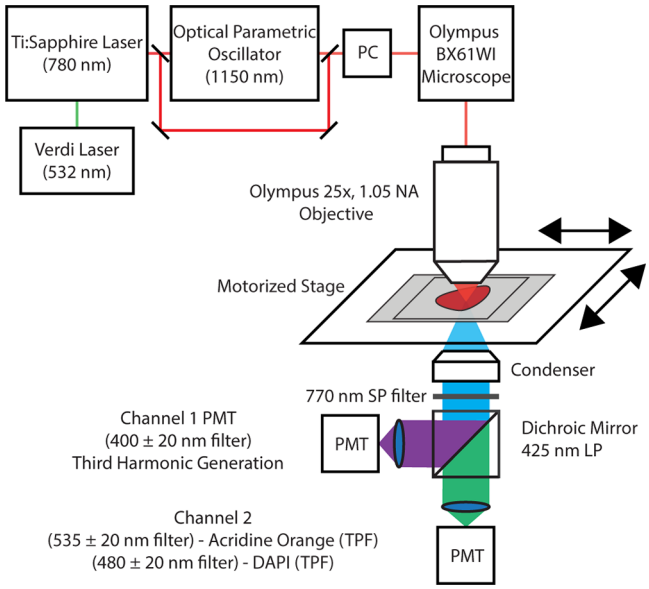

Figure 2. Experimental THGISC imaging setup. Abbreviations: PC, power control; PMT, photomultiplier tube; TPF, two-photon fluorescence; SP, short-pass filter; LP, long-pass filter.

system consists of two tunable ultrafast laser sources coupled to an upright microscope base and scanning unit (FV1200 MPE, Olympus Canada Inc., Ontario, Canada): a Ti:sapphire laser (Mira 900F, Coherent, California, U.S.A.) and an optical parametric oscillator (Mira OPO, Coherent, California, U.S.A.). Switching between sources is automated through two motorized flip mounts (MFF101, Thorlabs, New Jersey, U.S.A.), while laser power is controlled using a custom motorized variable attenuator system operated by a custom Labview Program (National Instruments, Texas, U.S.A.). Laser power is measured directly before beam entrance to the microscope using a thermal power sensor (S175C/PM100D, Thorlabs, New Jersey, U.S.A.). The excitation light was directed at blood smear samples mounted on a high-speed motorized stage (H117, Prior Scientific, Massachusetts, U.S.A.) using a 25× 1.05 NA water immersion multiphoton objective (XLPL25XWMP, Olympus Canada Inc., Ontario, Canada). A 0.9 NA dry top lens condenser directed the output light to two forward detection photomultipliers (PMTs), enabling simultaneous trans detection of THG light along with two-photon dye fluorescence. Blood smears were first imaged with OPO excitation (1150 nm, 150 mW) to collect THG emission (380−420 nm filter, ET400/40X, Chroma Technology, Vermont, U.S.A.). Two-photon fluorescence was then excited with the Ti:sapphire laser (780 nm, 80 mW) to enable detection of DAPI (460−500 nm filter, BA460-500, Olympus Canada Inc., Ontario, Canada) and acridine orange (515−555 nm filter, BA515-555, Olympus Canada Inc., Ontario, Canada). THG was separated from fluorescence using a dichroic mirror (T425LPXR, Chroma Technology, Vermont, U.S.A.). An edge-pass infrared blocking filter (FF01-770/SP32, Semrock, New York, U.S.A.) was placed immediately after the condenser to ensure complete blocking of excitation light at the detection PMTs. Samples were imaged using a 248 nm *X*−*Y* pixel size, 2 μs pixel dwell time, resulting in a 1 s frame time for a 1024 × 1024 pixels image.

Image Analysis. THG and dye fluorescence images were first registered using the pairwise FIJI stitching plug-in[25] to ensure overlap of features. For the cultured parasite experiments, a graphical user interface (GUI) MATLAB application was used to establish overlap of detected parasites between the THG and dye channels. First, an intensity threshold was used for each channel to create a binary image representing the hemozoin and parasite nuclei locations. Morphological dilation with a disk structural element was then used in each channel to ensure that overlapping signals from the same parasite were counted as one using the MATLAB functions “strel” and “imdilate”. The parasites in each channel were then counted with the “bwconncomp” function and compared. The GUI application is available upon request.

Malaria detection in patient blood was conducted using a custom GUI MATLAB application (Figure S1). First, a smoothing Gaussian filter (“imgaussfilt” function) was applied to the THG image to prepare for segmentation. A circular Hough transform (“imfindcircles” function) was then used to detect each individual red blood cell and establish a total cell count per image. Within the same channel, a threshold intensity was selected to locate potential parasites from their nearly saturated hemozoin signal. The centroids of these locations were found using the “regionprops” function, which were then referenced to the detected RBCs to verify that the hemozoin was located within an RBC. These cells were then declared as infected, and a total parasitemia % was calculated for each image and averaged for each patient sample. The GUI application is available upon request.

RESULTS AND DISCUSSION

Third-harmonic generation imaging enables a powerful malaria detection approach by providing a sensitive contrast mechanism that highlights both parasite-produced hemozoin and erythrocytes within the same detection channel. Hemoglobin, the oxygen transport protein that is ubiquitous within red blood cells, presents a resonance-enhanced THG signal when the THG wavelength is tuned close to its Soret spectroscopic absorption band.[26,27] This property has

DOI: 10.1021/acs.analchem.8b04791
Anal. Chem. 2019, 91, 2216−2223

previously been exploited to examine and evaluate morphology of stored RBCs within blood bags.[28] Hemozoin, also known as β-hematin, is a biocrystal formed during the *Plasmodium* parasite's digestion of hemoglobin.[29] The digestion process releases free hematin, which is toxic to the parasite, resulting in the production of hemozoin as a detoxification mechanism. Owing to a similar resonance mechanism as hemoglobin, hemozoin has been found to be a very strong source of THG, generating signals over an order of magnitude higher than those of hemoglobin. By using THG exclusively as a contrast mechanism, it is possible to simultaneously detect RBCs via hemoglobin and malaria parasites via hemozoin with the segmentation between the two easily implemented due to the large signal difference.

As THG is a nonlinear optical effect that requires a tight diffraction-limited beam focus to achieve the necessary excitation power, its usage is incompatible with standard flow cytometry instrumentation which uses a wide focus to illuminate whole cells at lower power. However, by combining THG laser scanning microscopy with rapid motorized scanning, a high-throughput measurement can still be achieved without relying on flow processes. This approach brings the benefit of image-based cytometry which provides single-cell characterization, enabling us to monitor hemozoin on a subcellular level in addition to visualizing morphological cellular features. Once images of the sampled erythrocytes are obtained, simple image processing can be used to identify and count red blood cells and highlight potential infected ones via the significant hemozoin signal.

Validation Using Cultured Parasites. To establish our method as a practical means for malaria detection, it was imperative to characterize its performance using known controls. We first applied our technique to *P. falciparum* parasites cultured in packed red blood cells at three different lifecycle stages: ring (early trophozoite), trophozoite, and schizont stages. To validate our measurements, two-photon fluorescence (TPF) imaging was performed alongside THG imaging using two nuclear staining fluorescent dyes commonly used for malaria parasite detection, acridine orange (AO)[30] and DAPI (4′,6-diamidino-2-phenylindole).[31] By performing two-photon fluorescence microscopy with the same imaging system as for THG, it was possible to obtain a direct comparison for parasite numbers obtained for the same fields of view with both methods. Since healthy RBCs do not possess DNA, any fluorescence signal present within an RBC after staining could be attributed to the presence of parasite DNA. Both AO and DAPI are intercalating DNA dyes and yield increased fluorescence upon binding to DNA. To obtain efficient two-photon excitation of the fluorescent dyes, a Ti:sapphire laser source was used instead of the OPO, owing to its ability to generate excitation light at a lower wavelength (780 nm), closer to the peak of their two-photon absorbance.

Example images obtained from this study can be found in Figure 3 for the three different parasite stages examined, showing nearly exact overlap (white) between the parasite nuclei (green for AO and cyan for DAPI) and hemozoin (magenta) locations. It is important to note that the hemozoin is located within the malaria parasite's digestive vacuole, whereas the AO/DAPI signals originate from the parasite's nucleus. As such, these two signals are not completely colocalized depending on the parasites' spatial orientation. The PMT sensitivity for the THG channel was adjusted to clearly visualize the RBCs in addition to the hemozoin,

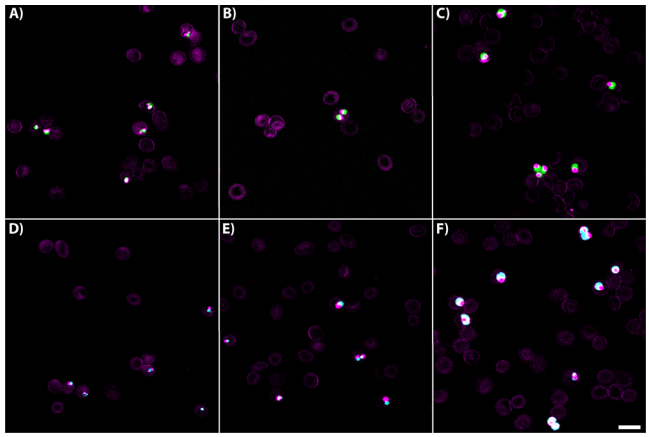

Figure 3. Validation of method performance using nuclear staining dyes on cultured *P. falciparum* parasites at the (A and D) ring, (B and E) trophozoite, and (C and F) schizont stages. Panels A−C were stained using acridine orange; panels D−F were stained using DAPI. Magenta, THG signal; green, TPF acridine orange; cyan, TPF DAPI. Scale bar: 10 μm. Separate channel images for panels A−C can be found in Figure S2, while separate channel images for panels D−F can be found in Figure S3.

resulting in a saturated signal associated with the presence of hemozoin due to its high intrinsic third-order nonlinear susceptibility. Using simple image processing, we determined the number of parasites per image obtained by THG and TPF for parasites stained with AO (Figure 4A) and DAPI (Figure 4B).

Using the slopes of the THG versus AO graphs, it could be seen that THGISC slightly underestimated ring (0.8186) and trophozoite (0.8170) numbers while matching the numbers obtained for schizonts (1.0085). The numbers obtained for DAPI-stained parasites showed an improvement across all stages, with the trophozoite and schizont slopes being significantly higher than for rings. The differences in parasite counts obtained by THGISC in comparison to those obtained from the fluorescent DNA probes could potentially be explained by a difference in focal planes between the two different laser sources used for excitation (780 nm Ti:sapphire vs 1150 nm OPO), which were manually switched for every experiment. As THG is an interface effect, it is significantly more sensitive to small changes in focal plane compared to bulk fluorescence. For earlier parasite stages (ring and trophozoite), it is possible that the THG excitation beam failed to encompass their smaller hemozoin crystals at the same focal plane in which fluorescence could still be seen from their nuclei.

To verify this hypothesis, an additional experiment (Figure 4C) was conducted using DAPI-strained trophozoites where the dye was excited using the same Ti:sapphire excitation source as before along with the OPO that is normally used for THG, this time manually switched to 1000 nm for each field, which was the shortest wavelength possible for this source. From Figure 4C, the precision of THGISC significantly improves (R^2 of 0.96 vs 0.88) when the same laser source is used for the comparison, demonstrating the importance of proper focal plane selection. This issue could potentially be resolved by automated autofocusing or the incorporation of three-dimensional image stacks for validation from which a maximum projection could be extracted instead of single images. However, in practical applications of our method,

DOI: 10.1021/acs.analchem.8b04791
Anal. Chem. 2019, 91, 2216−2223

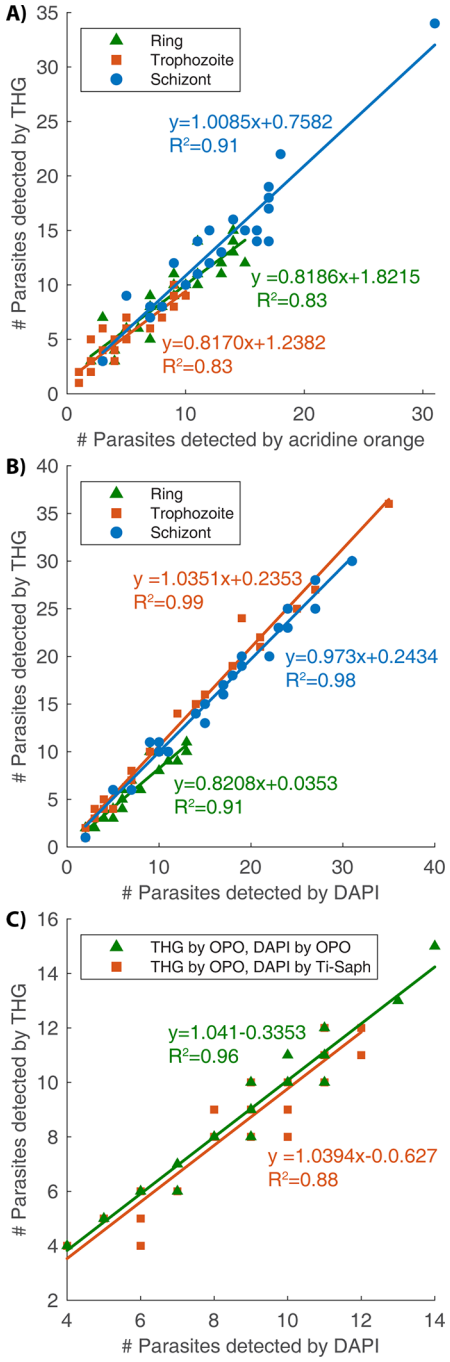

Figure 4. Results of method validation using fluorescent nuclear staining dyes on three different parasite lifecycle stages: ring, trophozoite, and schizont. Number of parasites obtained by our THG method vs no. of parasites detected by TPF using (A) acridine orange, (B) DAPI, and (C) DAPI with same/different excitation sources for comparison for trophozoites only. A linear regression best fit line was calculated for each data set (solid lines). N = 20−25 fields for each parasite stage.

proper focusing using the THG image channel directly should minimize false negatives due to this effect. We implemented this approach for our patient study.

Proof of Concept Using Whole-Blood Samples from Malaria Patients. To characterize our method for potential clinical applications, we conducted THGISC screening of whole blood obtained from malaria patients. For each patient, parasite count was first established at the point of origin by microscopy of thick blood films. Parasite count was conducted in thick MBF, and the estimated white blood cell count of the patient (8000) was used in determining the parasitemia in parasite per microliter count[32] (eq 1):

$$\frac{n_{\text{parasites}}}{\mu\text{L}} = \frac{n_{\text{parasites}}}{n_{\text{white blood cells}}} \times \frac{8000 \text{ white blood cells}}{\mu\text{L}} \quad (1)$$

Using THGISC, parasite counts were established using unlabeled methanol-fixed thin blood smears to determine a percentage of parasitemia for each patient. Parasitemia was determined using eq 2:

$$\%\ \text{parasitemia} = 100 \times \frac{n_{\text{infected RBCs}}}{n_{\text{total RBCs}}} \quad (2)$$

An example of images obtained from two different patients can be found on Figure 5. We established a direct comparison for

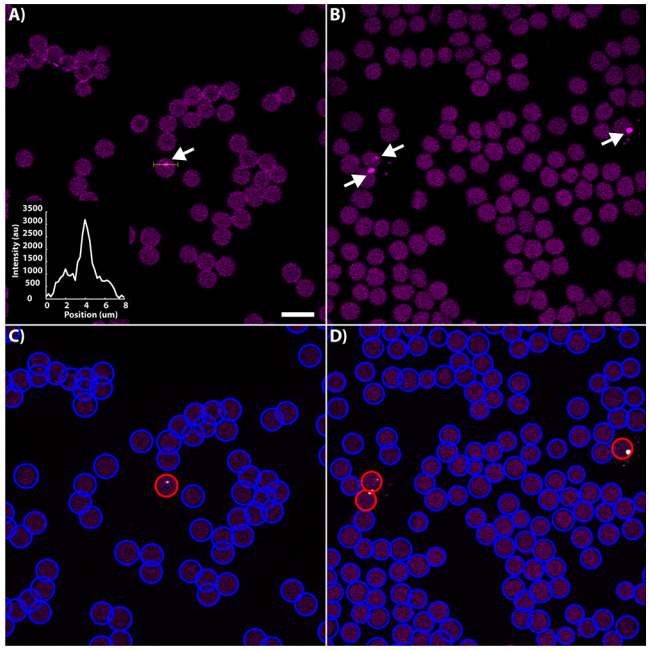

Figure 5. Raw and processed THGISC images for malaria detection in patient blood. (A and B) Malaria parasites (arrows) detected in whole-blood smears of two malaria patients. Inset: intensity cross section through red blood cell and hemozoin THG signals. (C and D) Red blood cell segmentation and hemozoin detection for images in panels A and B. Scale bar: 10 μm.

the % parasitemia obtained from our technique against the parasites per microliter that were previously clinically determined, which can be found on Figure 6. The relationship between the two methods can be seen to be very linear (R^2 of 0.96), demonstrating that malaria detection by THGISC provides comparable performance to the classical method of malaria detection.

The larger variation between figures obtained for patients having smaller parasite counts could potentially be explained by parasite reproduction during transit from Nigeria to Canada along with variation in sampling during preparation of the blood films. To obtain accurate results for smaller parasite counts, it is critical for the erythrocytes to be set in a proper single layer with the blood homogeneously mixed to increase the chances of finding single isolated parasites.

DOI: 10.1021/acs.analchem.8b04791
Anal. Chem. 2019, 91, 2216−2223

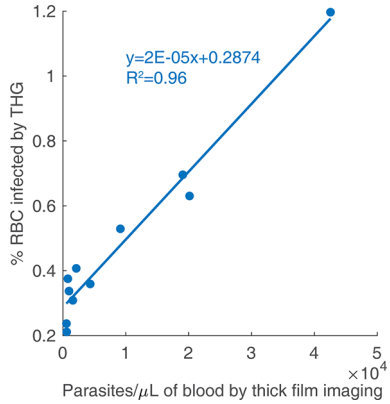

Figure 6. Results of method characterization using patient samples. *N* = 11 patients. The percentage of infected RBCs is comparable to parasitemia obtained via imaging of thick films. A linear regression best fit line was calculated (solid line).

Thanks to the use of automated scanning, the number of fields examined by THGISC could also be increased to cover most of the blood smear to increase detection probability in patients with low parasitemia. Assuming that the parasitemia rate is constant throughout a blood sample, the probability of finding a small parasite count within the millions of uninfected blood cells should follow a Poisson distribution. The higher throughput enabled by our method could allow examiners to sample significantly more fields than is normally possible due to labor constraints, which could increase the overall probability of finding at least one parasite in an entire blood smear. Such an approach could also be beneficial for parasite screening in populations to find potential asymptomatic carriers, an important checkpoint on the road to complete malaria eradication.[33] In addition, automated scanning removes the subjectivity of manual malaria blood smear reading by microscopists, while increasing the screening throughput.

The main drawback of the technique is the requirement for an ultrafast mode-locked excitation laser source for THG imaging which carries a significant initial expense. However, while a research grade tunable OPO was used in our demonstration, a much less expensive setup using a single-wavelength fiber laser based setup could provide a more economical option.[34] With the rapid progress in laser oscillator development and optimization, it is conceivable to expect such laser sources to become more widely available and accessible. Other than cost, the power requirement of the excitation laser must also be considered, rendering this method more viable for use in larger hospitals and clinics where such power can be reliably present. In such locations, a quantitative and easy-to-use higher throughput method would be highly advantageous for routinely tracking patient parasitemia throughout treatment, allowing earlier health care interventions.

Another limitation of the technique is the throughput obtained via laser scanning cytometry in comparison to flow cytometry. While much faster than manual counting, a higher throughput would be desirable. Due to the nature of THG as an interface effect arising from the Gouy phase shift, the emitted signal is maximized when the sample being imaged is on the same physical scale as the laser beam.[35] For hemozoin crystals, this requires diffraction-limited beam sizes to maximize sensitivity.[20] To incorporate this approach into a flow cytometry instrument, a high-speed line scanner could potentially be adapted to continuously scan incoming RBCs. However, this would require a very tight focus of the cell flow in the axial dimension to avoid focal plane issues. Another potential solution would be the utilization of scanned Bessel beams to increase the available depth of field to ensure that parasites are detected along all axial positions in each RBC. However, a theoretical evaluation of the application of Bessel beams to THG imaging showed that it would potentially require significantly more excitation power than the standard Gaussian beams typically used in THG microscopy, which would bring additional challenges to the practical implementation.[36] Biologically, the absence of hemozoin in the very early ring stages of *Plasmodium* parasites (less than 6 h)[37] may be missed by THG and could explain the slightly reduced detection compared with TPF.

Malaria detection by THGISC shows promising results as compared to the current gold standard, light microscopy; however, several improvements could be made to enhance the measurements. While blood smears were prepared in methanol for each patient sample to ensure sample preservation for the entire batch after receiving of the shipment, direct measurements without fixation could provide a benefit in sensitivity. In live samples, red blood cells present a more standardized shape, resulting in better image segmentation. In addition, live samples present a lower background signal due to a reduced number of THG-emitting particles that can often be introduced during sample processing.

Treatment options for malaria patients typically consist of artemisinin-based combination therapies (ACT) where an artemisinin derivative is combined with a quinine derivative. The specific combinations, treatment duration, and dosage depend on patient factors such as endemicity, age, weight, pregnancy, and immunocompromised status, in addition to clinical diagnosis. According to the WHO,[38] symptomatic malaria patients with no signs of severity or organ dysfunction are categorized as “uncomplicated malaria”, whereas “severe malaria” is defined with signs of severity and/or signs of vital organ dysfunction. It has been reported that some patients may be symptomatic at parasitemia levels as low as 0.002%, whereas patients that have developed a partial protective immunity owing to repeated exposure only show symptoms above parasitemia of 0.2%.[39] The WHO defines hyperparasitemia as >4%, a level which increases the risk of deterioration from uncomplicated to severe malaria. At a parasitemia >10%, the WHO considers the case to be severe malaria even if there is no evidence of vital organ dysfunction. We have demonstrated malaria detection at physiological levels ranging from 0.2% to 1.2%, consistent with detection using Giemsa-stained blood smear imaging. However, our method demonstrates an automated higher throughput approach in comparison to manual counting by microscopists.

Current developments in adaptive optics and three-photon fluorescence instrumentation have resulted in significant improvements in deep tissue imaging, with some commercial objectives allowing imaging at depths of up to 8 mm. Given such progress, it could be possible to apply THG-based malaria detection in vivo with imaging conducted directly in blood vessels through patient skin with epi-based detection. Such an approach was previously used for conducting human leukocyte cytometry by using THG transdermally.[40]

DOI: 10.1021/acs.analchem.8b04791
Anal. Chem. 2019, 91, 2216−2223

CONCLUSION

We developed a new optical detection method and demonstrated that it is a viable tool for malaria detection. By combining the sensitivity of THG imaging with high-speed motorized scanning and image processing software, malaria detection at the single red blood cell level can be achieved. The technique relies on intrinsic contrast obtained from the third-order susceptibilities of hemoglobin and hemozoin to obtain both cytometry of red blood cells and detection of malaria parasites in a single channel. Unlike traditional methods, our approach does not require any labels or any preparation beyond a simple blood smear. In addition, thanks to the automated image processing, parasitemia counts can be rapidly determined in an objective manner without requiring skilled labor. While the method was shown to be sensitive to proper focusing, this could be remedied with the use of an autofocus module.

In control measurements, THGISC showed good linearity and comparable results to parasite counts obtained by two-photon fluorescence of parasite DNA stains, with a slight underestimation of smaller parasites from earlier stages (ring and trophozoite). In direct application to blood smears obtained from confirmed malaria patients, the technique showed great linearity and comparable performance to standard thick blood smear measurements. The ability to easily and rapidly determine parasitemia offers potential not only for the easy confirmation of malaria diagnoses following symptoms, but also the tracking of treatment progress in existing patients, potentially allowing physicians to adjust medication and dosage for each individual. The technique could also be used to assist in the development of new antimalarial drugs, some of which have been theorized to be actively blocking hemozoin formation, resulting in a fatal outcome for the parasite.[41]

ASSOCIATED CONTENT

Supporting Information

The Supporting Information is available free of charge on the ACS Publications website at DOI: 10.1021/acs.analchem.8b04791.

MATLAB application for red blood cell counting and hemozoin detection by THGISC image analysis and validation of method performance using acridine orange and DAPI nuclear staining (PDF)

AUTHOR INFORMATION

Corresponding Author

*E-mail: paul.wiseman@mcgill.ca.

ORCID

Paul W. Wiseman: 0000-0002-5732-2858

Notes

The authors declare no competing financial interest.

ACKNOWLEDGMENTS

The authors gratefully acknowledge Discovery Grant support from the Natural Sciences and Engineering Research Council of Canada for P.W.W. (RGPIN-2018-05005) and E.G. (RGPIN-2017-05009). A.K. would like to acknowledge the Fond de Recherche du Quebec—Nature et Technologies for scholarship support. The authors thank the Bio Ventures for Global Health Organization for helping establish this collaboration. We thank the Lagos State Ministry of Health for approving the use of Health Facilities in Ikorodu, Lagos State, Nigeria where samples for this study were obtained as well as the management and staff of Ijede General Hospital and Imota Primary Health Centre, Ikorodu, Lagos, Nigeria.

REFERENCES

(1) Phillips, M. A.; Burrows, J. N.; Manyando, C.; van Huijsduijnen, R. H.; Van Voorhis, W. C.; Wells, T. N. C. *Nat. Rev. Dis Primers* **2017**, *3*, 17050.
(2) *World Malaria Report 2017*; World Health Organization: Geneva, Switzerland, 2017.
(3) Miller, L. H.; Ackerman, H. C.; Su, X. Z.; Wellems, T. E. *Nat. Med.* **2013**, *19* (2), 156−67.
(4) White, N. J.; Pukrittayakamee, S.; Hien, T. T.; Faiz, M. A.; Mokuolu, O. A.; Dondorp, A. M. *Lancet* **2014**, *383* (9918), 723−735.
(5) Cowman, A. F.; Healer, J.; Marapana, D.; Marsh, K. *Cell* **2016**, *167* (3), 610−624.
(6) Mathison, B. A.; Pritt, B. S. *J. Clin. Microbiol.* **2017**, *55* (7), 2009−2017.
(7) Hathiwala, R.; Mehta, P. R.; Nataraj, G.; Hathiwala, S. *J. Infect Public Health* **2017**, *10* (6), 824−828.
(8) Wilson, M. L. *Arch. Pathol. Lab. Med.* **2013**, *137* (6), 805−11.
(9) Britton, S.; Cheng, Q.; McCarthy, J. S. *Malar. J.* **2016**, *15*, 88.
(10) Kolluri, N.; Klapperich, C. M.; Cabodi, M. *Lab Chip* **2018**, *18* (1), 75−94.
(11) Ragavan, K. V.; Kumar, S.; Swaraj, S.; Neethirajan, S. *Biosens. Bioelectron.* **2018**, *105*, 188−210.
(12) Coronado, L. M.; Nadovich, C. T.; Spadafora, C. *Biochim. Biophys. Acta, Gen. Subj.* **2014**, *1840* (6), 2032−41.
(13) Delahunt, C.; Horning, M. P.; Wilson, B. K.; Proctor, J. L.; Hegg, M. C. *Malar. J.* **2014**, *13*, 147.
(14) Pirnstill, C. W.; Cote, G. L. *Sci. Rep.* **2015**, *5*, 13368.
(15) Lukianova-Hleb, E. Y.; Campbell, K. M.; Constantinou, P. E.; Braam, J.; Olson, J. S.; Ware, R. E.; Sullivan, D. J., Jr.; Lapotko, D. O. *Proc. Natl. Acad. Sci. U. S. A.* **2014**, *111* (3), 900−5.
(16) Lukianova-Hleb, E.; Bezek, S.; Szigeti, R.; Khodarev, A.; Kelley, T.; Hurrell, A.; Berba, M.; Kumar, N.; D'Alessandro, U.; Lapotko, D. *Emerging Infect. Dis.* **2016**, *22* (2), 344−344.
(17) Burnett, J. L.; Carns, J. L.; Richards-Kortum, R. *Biomed. Opt. Express* **2015**, *6* (9), 3462−74.
(18) Weigelin, B.; Bakker, G. J.; Friedl, P. *J. Cell Sci.* **2016**, *129* (2), 245−55.
(19) Belisle, J. M.; Costantino, S.; Leimanis, M. L.; Bellemare, M. J.; Bohle, D. S.; Georges, E.; Wiseman, P. W. *Biophys. J.* **2008**, *94* (4), L26−8.
(20) Tripathy, U.; Giguere-Bisson, M.; Sangji, M. H.; Bellemare, M. J.; Bohle, D. S.; Georges, E.; Wiseman, P. W. *Anal. Bioanal. Chem.* **2013**, *405* (16), 5431−40.
(21) Pozarowski, P.; Holden, E.; Darzynkiewicz, Z. *Methods Mol. Biol.* **2006**, *319*, 165−92.
(22) Pozarowski, P.; Holden, E.; Darzynkiewicz, Z. *Methods Mol. Biol.* **2012**, *931*, 187−212.
(23) Han, Y.; Gu, Y.; Zhang, A. C.; Lo, Y. H. *Lab Chip* **2016**, *16* (24), 4639−4647.
(24) Trager, W.; Jensen, J. *Science* **1976**, *193* (4254), 673−675.
(25) Preibisch, S.; Saalfeld, S.; Tomancak, P. *Bioinformatics* **2009**, *25* (11), 1463−5.
(26) Chang, C. F.; Yu, C. H.; Sun, C. K. *Journal of biophotonics* **2010**, *3* (10−11), 678−85.
(27) Clay, G. O.; Millard, A. C.; Schaffer, C. B.; Aus-Der-Au, J.; Tsai, P. S.; Squier, J. A.; Kleinfeld, D. *J. Opt. Soc. Am. B* **2006**, *23* (5), 932−950.
(28) Saytashev, I.; Glenn, R.; Murashova, G. A.; Osseiran, S.; Spence, D.; Evans, C. L.; Dantus, M. *Biomed. Opt. Express* **2016**, *7* (9), 3449−3460.
(29) Egan, T. J. *J. Inorg. Biochem.* **2002**, *91* (1), 19−26.

DOI: 10.1021/acs.analchem.8b04791
Anal. Chem. 2019, 91, 2216−2223

(30) Shute, G. T.; Sodeman, T. M. *Bull. World Health Organ.* **1973**, *48* (5), 591−596.
(31) Hyman, B. C.; Macinnis, A. J. *J. Parasitol.* **1979**, *65* (3), 421−5.
(32) *DPDx - Laboratory Identification of Parasites of Public Health Concern. Determination of Parasitemia*; Centers for Disease Control and Prevention: Atlanta, GA, 2014.
(33) Krampa, F. D.; Aniweh, Y.; Awandare, G. A.; Kanyong, P. *Diagnostics* **2017**, *7* (3), 54.
(34) Millard, A. C.; Wiseman, P. W.; Fittinghoff, D. N.; Wilson, K. R.; Squier, J. A.; Muller, M. *Appl. Opt.* **1999**, *38* (36), 7393−7397.
(35) Beaurepaire, E.; Débarre, D.; Olivier, N. THG Microscopy of Cells and Tissues: Contrast Mechanisms and Applications. In *Second Harmonic Generation Imaging*; CRC Press: Boca Raton, FL, 2016; pp 70−99.
(36) Olivier, N.; DeBarre, D.; Mahou, P.; Beaurepaire, E. *Opt. Express* **2012**, *20* (22), 24886−902.
(37) Delahunt, C.; Horning, M. P.; Wilson, B. K.; Proctor, J. L.; Hegg, M. C. *Malar. J.* **2014**, *13*, 147.
(38) *Guidelines for the Treatment of Malaria*; World Health Organization: Geneva, Switzerland, 2015.
(39) Hanscheid, T. *Clin. Lab. Haematol.* **1999**, *21* (4), 235−45.
(40) Wu, C. H.; Wang, T. D.; Hsieh, C. H.; Huang, S. H.; Lin, J. W.; Hsu, S. C.; Wu, H. T.; Wu, Y. M.; Liu, T. M. *Sci. Rep.* **2016**, *6*, 37210.
(41) Kumar, S.; Guha, M.; Choubey, V.; Maity, P.; Bandyopadhyay, U. *Life Sci.* **2007**, *80* (9), 813−28.

DOI: 10.1021/acs.analchem.8b04791
Anal. Chem. 2019, 91, 2216−2223